Functional data analysis of single-trial auditory evoked potentials recorded in the awake rat

Ondřej Pokora[a,*], Jan Koláček[a], Tzai-Wen Chiu[b], Wei Qiu[c]

[a] *Department of Mathematics and Statistics, Faculty of Science, Masaryk University, Kotlarska 2, Brno, 61137, Czech Republic*
[b] *Department of Biological Science and Technology, National Chiao Tung University, 75 Bo-Ai Street, Hsinchu, Taiwan*
[c] *Auditory Research Laboratory, State University of New York, 107 Beaumont Hall, Plattsburgh, New York 12901, USA*

Abstract

Evoked potentials (EPs) reflect neural processing and are widely used to study sensory perception. However, methods of analyzing EP have been limited mostly to the conventional ensemble averaging of EP response trials to a repeated stimulus, and less so to single-trials analysis. Here we applied a new approach – functional data analysis (FDA) – to study auditory EP in the rat model of tinnitus, in which overdoses of salicylate (SS) are known to alter sound perception characteristically, as the same way as in humans. Single-trial auditory EPs were analyzed, after being collected on a daily basis from an awake rat, which had been surgically implanted with intracranial electrodes over its auditory cortex. Single-trial EP integrals were generated with sound stimuli presented systematically over an intensity range. The results were approximated using the cubic spline to give sets of smoothed response-level functions for each of the three sounds. Comparisons between daily intensity-series for each sound type were done using cross-distance measures based on the response-level functions in both the original form and the first-derivative form. From the results of FDA, the first-derivative form was found to provide a clearer separation, when EP data were compared between SS and the Control groups. This is also true when the daily data were compared within the more variable SS-group itself. In addition, at the high intensity region where SS-action is presumably strong, we also observed characteristic changes in two statistical parameters, mean and skewness, of the cross-distance representations. Results suggested that FDA is a sensitive approach for EP studies, and it can become a powerful tool for the research in neural science, particularly neuropharmacology.

Keywords: auditory cortex, evoked potential integral, functional data, salicylate, semimetric, tinnitus

*Corresponding author
Email addresses: pokora@math.muni.cz (Ondřej Pokora), kolacek@math.muni.cz (Jan Koláček), twchiu@g2.nctu.edu.tw (Tzai-Wen Chiu), wei.qiu@plattsburgh.edu (Wei Qiu)

1. Introduction

1.1. Auditory evoked potential and current methods of analysis

Auditory evoked potentials (EPs, or the electrophysiological manifestations of sound-induced neural responses), are highly correlated with sound perception, for review see Alho (1992); Bidelman (2017). EP is typically recorded through surface electrodes placed far-field (or some times near-field) to the generator sources in the brain. The ongoing neural activities (or EEG) especially strong in the awake state, often mask the EP time-locked to the stimulus. To extract EP from the background EEG signal, the traditional approach is by ensemble averaging single-trial responses to repeated stimuli. The mean EP signal is then studied. A more recent approach is the application of adaptive filter that allows extraction of single-trial EP from the ongoing EEG signal (Qiu et al., 2006). Given single-trial EPs, additional information (e.g., variance) can be derived apart from the mean EP. Such additional information is increasingly noted to be valuable regarding neural mechanisms underlying perception (Faisal et al., 2008; Neri, 2010; Bernasconi et al., 2011).

1.2. Tinnitus and EP studies

Tinnitus is a well-known abnormal perception of sound in the absence of acoustic stimuli (Jastreboff, 1990); for review see Roberts et al. (2010). Around 15 % of the general population experience the condition of chronic tinnitus and, in some cases, the symptom is strong enough to affect their quality of life (Levi and Chisin, 1987; Jastreboff, 1990; Langguth et al., 2013). Tinnitus often requires medical intervention for its management but no effective cure is available, as mechanisms underlying tinnitus perception remain obscure (Coles, 1984; Heller, 2003). The hypothesis generally accepted regarding its pathophysiology is one that tinnitus is a side effect of an elevated central gain following cochlear damages (Noreña, 2011; Noreña and Farley, 2013). Direct evidence, in electrophysiology or EP in particular, is not yet available to demonstrate a causal link between impaired sensory input and elevated central gain. To study such link, animal models (rather than human subjects) are used widely for the study of experimental tinnitus for obvious reasons.

One popular model is the overdose with sodium salicylate (SS). SS, the active component of the pain-killer aspirin, is known to induce a tinnitus percept as reported by humans, and likely also in animals based on their altered behaviors (Boettcher and Salvi, 1991); for review see Cazals (2000). The current opinion on the sequence of events of experimental tinnitus following an SS-overdose is the following: (a) SS suppresses auditory inputs at the sensory receptors (by inactivating outer hair cells in the inner ear) and neuro-homeostasis is subsequently disturbed, (b) the central gain control system in the brain would automatically compensate the loss in inputs by increasing its gain to amplify the weakened sensory signals, (c) likely due to imperfect compensations, the central gain control system not only over-amplifies silence (resulting in the perception of nonexisting phantom sound or a condition clinically called tinnitus), but also loud sounds (clinically called hyperacusis). In rats, the experimental tinnitus after a single SS-overdose can last for several hours, providing a good opportunity to study SS-induced changes in auditory EP in a reversible way on a daily basis, often over extended periods up to weeks.

In a previous study on awake rats, we have reported the changes of auditory EP during SS-induced tinnitus using intra-cranially near-field electrodes implanted over the cortex (Wan et al., 2015). What we found of interest are the large daily variations in EP to sound particularly after SS treatment. What could be derived from the response variance remained unclear as the method of analysis at that time was based on mean EPs and a response-level function generated by parametric curve fitting. In the present study, we wanted to use a novel approach called functional data analysis to extract additional information from EP in order to tell more about the changes of neural mechanisms after SS-treatment.

1.3. Functional data analysis

Functional data analysis (FDA) is a relatively recent topic in statistics and it has never been applied to study evoked potentials (EPs) from the brain. FDA is based on the concept of a functional random variable, which is a random variable taking values in infinite dimensional space. Natural examples of a functional random variable are the random curves and surfaces, but the concept itself covers also more complex objects (Ramsay and Silverman, 2005; Ferraty and Vieu, 2006). Realizations of the functional random variable are called the functional data, which are treated as members of infinite dimensional space.

Here, FDA is used in the analysis of evoked potentials for the first time. Specifically, it allows the categorization of single-trial responses that have typically large inter-trial variance (in both the time waveform and the strength of response) as noted particular when recording from awake animals. The basic idea behind FDA is first to express discrete observations arising from EP in the form of a function (to create functional data) that represents a single observation and then to draw modeling information from a collection of functional data by applying statistical concepts based on multivariate data analysis.

The usefulness of the functional approach has been recognized in different fields of science. A systematic review of using FDA in practice has been given by Ullah and Finch (2013) and Wang et al. (2016). Earlier on, Ramsay (1982, 1988) presented some arguments for choosing FDA. Ramsay and Dalzell (1991) gave a number of practical considerations for functional data, for example, (a) smoothing and interpolation procedures can yield functional representations of a finite set of observations; (b) it is more natural to think through modeling problems in a functional form; and (c) the objective of an analysis can be functional in nature, as would be the case if finite data are used to estimate an entire function, its derivative, or other functionals.

The FDA approach is highly flexible in several respects, when applied to our case of EPs. First, the stimulus levels for generating EPs do not need to be equally spaced or fixed across trials. Second, FDA also does not require that values observed across stimulus levels are independent. Furthermore, FDA allows the extraction of additional information contained in the function and its derivative, which is not available in the traditional statistical analyses (Ferraty et al., 2006; Mas and Pumo, 2009). Finally, in FDA, the whole curve or functional data, is treated as a single entity, the repeated measurements are therefore not required to fulfill any special correlation structure.

The move from a real random variable to a functional one brings several challenges. One of them is the choice of distance measure. Such choice is not straightforward (unlike that in finite dimensional setting) and it has a noticeable

impact on properties of the estimates. Ferraty and Vieu (2006) proposed the use of semimetrics as the distance measure and introduced three classes of semimetrics based on: (a) derivative, (b) functional principal component analysis, and (c) partial least squares regression. The use of semimetrics instead of metrics appears to yield good practical results, but it poses theoretical challenges as the theory of semimetric space is less straightforward compared to that of metric space. In practice, the choice of an appropriate semimetric for the data seems crucial. Derivative-based semimetrics are suitable for relatively smooth data, as in our case of EPs, whereas the other two kinds of semimetrics work better for data that are comparatively rough or noisy (Benhenni et al., 2007).

In the present study, we have applied the novel FDA approach to analyze the sound-evoked responses in the awake rat before and after SS overdoses repeated on a daily basis. EPs to a battery of sounds were recorded through surgically pre-implanted intra-cranial electrodes, and later analyzed on single-trial basis.

2. Methods

2.1. Electrophysiology and surgery

An adult rat (Sprague-Dawley strain, ca. 300 gm body weight) was first anesthetized (inhalation of 3% isofluorane) to undergo aseptic surgery for the exposure of the cortical areas (temporal and frontal) on one side. A pair of silver-wire electrodes (Teflon coated, 0.005 inch diameter) was implanted (one over the auditory area as the active lead, and the other over the frontal area as the reference lead). Wires leaving the electrodes were attached to a mini-connector which was fixed on the top of the skull (with Histoacryl and reinforced with dental cement). The resected skin was closed with fine suture and the animal was returned to the rearing cage and allowed to rest for 10 days. Post-surgical pain was controlled by pain-killer (ibuprofen), skin wounds treated with antibiotic ointment, and the animal checked for possible infections every day.

Starting on day-10 before SS treatment, the rat was placed inside a sound-treated behavioral observation chamber for 4 days (4 hrs/day) to adapt to the environment. Starting on day-7 before SS treatment, the animal received for 6 consecutive days a daily injection of the drug-carrying vehicle (PBS solution) to establish the Control condition. Electrophysiological measurements were made during a period of 4 hours post-injection. We recorded the EP responses to three kinds of sounds: single click (or acoustic transient), tone burst of 10 or 16 kHz. At the end of Control measurements, the rat was allowed to rest for 1 day before similar EP recordings were carried out under SS treatments in the following 8 days. The rat was therefore experimented on for a total of 14 days.

During recordings, the miniature connector plug on the rat skull was connected to two chronic head stages (RA4PA, TDT), and fed to a 32-bit neurophysiology base station (RZ5, TDT). The control of experimental equipment was done through an OpenEx software (TDT). Signals were amplified, band-pass filtered (3–3000 Hz), monitored in real time and digitized (12 kHz sampling rate, 16-bit resolution) before storage in computer.

Tone bursts (10-msec duration, 2.5 msec rise/fall time) and single click (10 us width) were presented through a free-field speaker (EF1, TDT) located at the ceiling of the sound-treated chamber. In the case of tone bursts, the frequency was randomly chosen from a user menu (10 or 16 kHz). Sound intensity was

systematically presented across an intensity range of 90 dB (−15 to 75 dB SPL, 5 dB steps, from low to high, 81 repetitions at each intensity). Sound intensity was calibrated at the site of animal (using a precision microphone system, B&K 5113). Responses to each sound presentation (or trial) were collected for a duration of 1 sec (400 msec before, 600 msec after stimulus onset, with 2 sec inter-trial intervals). A total of 79 trials were collected during a single session at a fixed frequency and intensity. For a given stimulus, 19 sessions recorded to the sound at different intensities formed an intensity series, from which the response-level functions were derived.

Experimental procedures were approved by the Institutional Laboratory Animal Care and Use Committee of National Chiao-Tung University in compliance with the Guide for the Care and Use of Laboratory Animals.

2.2. Data analysis

Trials with the root-mean-square (RMS) larger or smaller than the grand mean of the RMS across total trials plus or minus the 3 times of the standard deviations (mostly due to unexpected animal movements) were rejected. No more than 2 trials were rejected from each session. As a result, 79 trials of EP were analyzed for each session. EP integrals were then computed for a time-window of 34 msec (14 to 47 msec post-stimulus onset. Details are shown in Fig. 1.

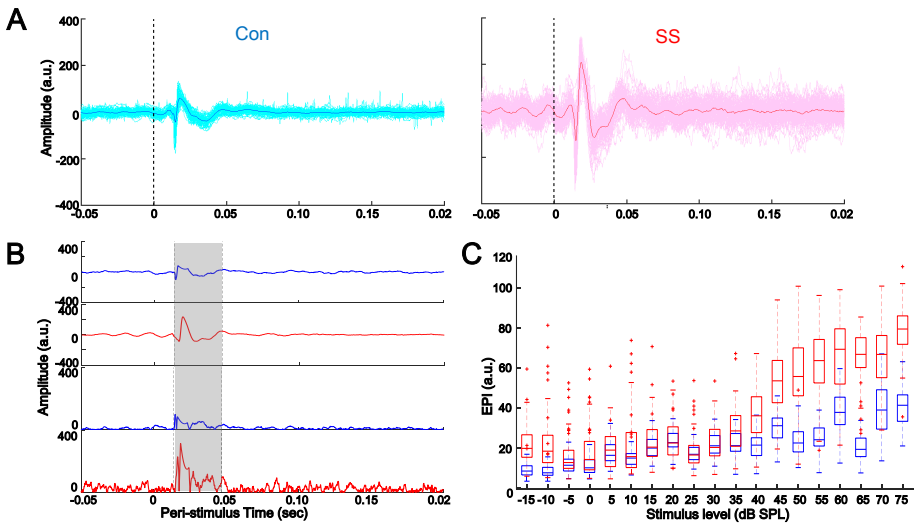

Figure 1: Examples of EP time waveforms (A) obtained in a single session under the Control (blue), and SS condition (red), showing the superposition of all 79 trials for each session. (B) A single-trial EP time waveform is shown for the Control (blue), and SS condition (red), accompanied by their full-wave rectified waveform. Grey areas mark the time-window of the EP integral. (C) Boxplots of the distribution of EP integral (EPI) data across an intensity range of 90 dB (Control: blue, SS: red).

In each intensity-series to a given sound, EP integral data were chosen according to their acquisition order in the individual sessions. For example, to obtain the first set of 19 intensity-driven EP integral values across intensity, all

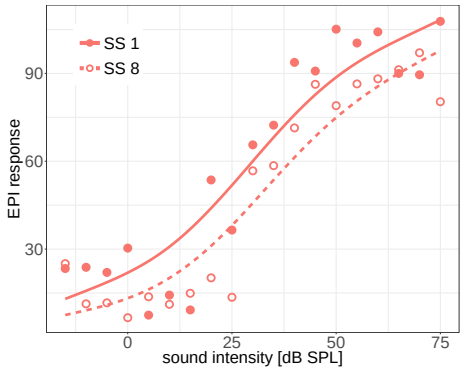

Figure 2: Two typical courses of the EP integral (EPI) response in dependency on the sound intensity. The analyzed EPI data (circles and discs) are accompanied by the corresponding cubic smoothing splines. The discs show a representative single-trial EPIs to click sound (SS, day-1), the corresponding spline is plotted as solid curve. The circles show a representative single-trial EPIs to click sound (SS, day-8), the corresponding spline is plotted as dashed curve.

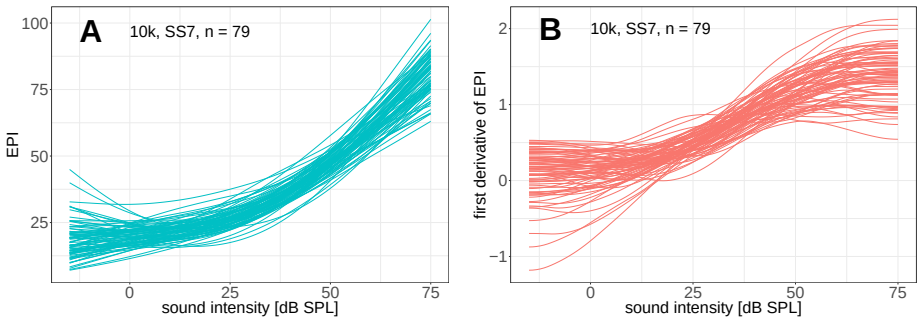

Figure 3: Examples of response-level functions (superposition of 79 spline-fitted curves that constitute a complete intensity-series) showing their shapes in dependency on the sound intensity. (A) Responses represent single-trial EP integrals (EPI) to 10 kHz tone (SS, day-7). (B) The corresponding first derivatives of the splines.

the first acquired EP integral values were chosen from the 19 sessions. A cubic spline algorithm was then applied to the set to generate a smooth response-level function. Two representative examples of the data and corresponding smoothing splines are depicted in Fig. 2. For each intensity series (which contained $79 \times 19 = 1\,501$ trials), a total of 79 curves were obtained. The first derivatives of the splines were subsequently computed. Finally, we computed the cross-distance for response-level functions represented in both forms: d_0 (original metric) and d_1 (semimetric based on the first derivative). Fig. 3 shows 79 splines and their first derivatives for the case of 10 kHz tone bursts (SS, day-7). The EP integral splines and their first derivatives for the complete analyzed dataset are shown in Supplementary Figs. S1 and S2. Mathematical details of the construction of the smoothing splines and the definitions of the used distances are given in Section 2.3.

2.3. Data smoothing and cross-distance computation

In general, the relation between a covariate x and a response Y is modelled as a smoothing spline $y = f(x)$ using the pairs (x_i, Y_i) of the data, $i = 1, \ldots, m$. In our case, the covariate x is represented by the sound intensity (x_i varies from -15 to 75 dB SPL in 5 dB steps). The single-trial EP integral plays the role of response Y.

The cubic smoothing spline, $f(x)$, is defined to be the minimizer of the functional

$$\sum_{i=1}^{m} \big[Y_i - f(x_i)\big]^2 + \lambda \int_{x_1}^{x_m} f''(x)^2 \mathrm{d}x \tag{1}$$

over the class of twice differentiable functions f. For the algorithm of the construction of the smoothing spline see, e. g., Reinsch (1967).

The smoothing spline does not necessarily interpolate the data points. In general, the particular values, x_i, of the covariate and the corresponding observed responses, Y_i, are linked by $Y_i = f(x_i) + \varepsilon_i, i = 1, \ldots, m$, where ε_i are realizations of the random errors. The parameter $\lambda > 0$ is the smoothing parameter, controlling the degree of smoothness of the regression function. This corresponds to the situation, where the covariate, x_i, is given and the observed response, Y_i, is the realization of some random variable linked with the value of x_i. The resulting smoothing spline, f, balances the size of the errors, ε_i, and the smoothness of the function linking the covariate and the response. In the case of the cubic smoothing spline, f, the second derivative, f'', becomes piecewise linear function. The larger the smoothing parameter is, the less sensitive it is to fluctuations in the data. The smoothing parameter can be determined by the generalized cross-validation method, see Craven and Wahba (1978) and Hastie and Tibshirani (1990).

Since the observations or EP integrals are assumed to be curves (i.e., response-level functions), a metric and a semimetric were constructed to represent the distance separation between two curves (note the smaller the cross-distance, the more similar are the two curves). Let f_1 and f_2 be two curves, specifically two cubic smoothing splines in our case. A well-known and widely-used distance between given curves f_1 and f_2 is the L_2-metric, $d_0(f_1, f_2)$. It is a nonnegative number, whose square is defined as the integral

$$d_0^2(f_1, f_2) = \int_{x_1}^{x_m} \big[f_1(x) - f_2(x)\big]^2 \mathrm{d}x. \tag{2}$$

Let us call this common metric as d_0-distance.

Similarly, a common way to build a semimetric between two curves is to consider the L_2-distance between the first derivatives of the curves. More precisely, given two curves f_1 and f_2, we define the d_1-distance $d_1(f_1, f_2)$ to be a nonnegative number, whose square is given by the integral

$$d_1^2(f_1, f_2) = \int_{x_1}^{x_m} \big[f_1'(x) - f_2'(x)\big]^2 \mathrm{d}x. \tag{3}$$

Note an important distinction between these two distances: the d_0-distance is a metric, whereas the d_1-distance is a semimetric. Hence $d_1(f_1, f_2) = 0$ does not necessarily imply $f_1 \equiv f_2$, i. e., two different curves can have zero d_1-distance. As an example, consider two identical curves with a vertical shift,

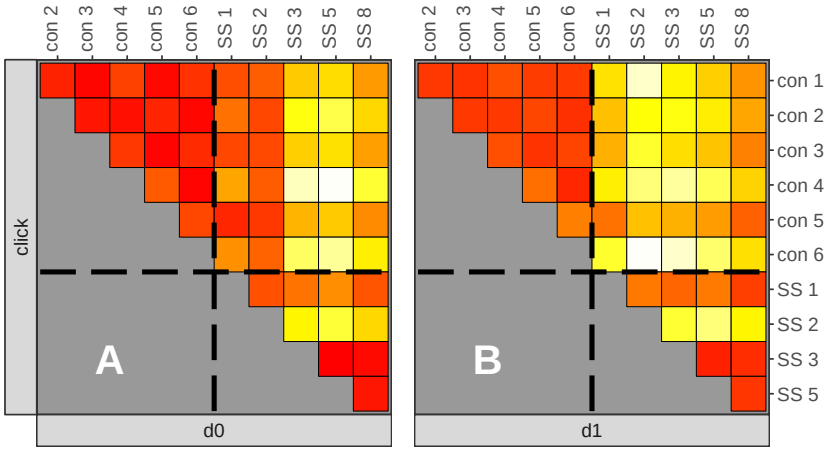

Figure 4: Pixel plots (or heatmaps) showing the results of the inter-series comparison between any two group-members of the Control and SS, color-coding median-disparity cross-distances histograms (redder color means larger similarity, brighter color means smaller similarity). Data are from click responses: 6 for Control, 8 for SS conditions, numerals on axes indicate the days of recording, and are arranged chronologically. (A) Heatmap of the results on d_0-cross-distances computed between pairs curves for all group-members. (B) Heatmap of results on d_1-cross-distances for the same data as in (A). Dashed lines divide the Control and SS groups for easy viewing. The corresponding cross-difference histograms are shown in Fig. 5.

$f_1 = f_2 + c$ for some constant $c \neq 0$. It is readily seen, that $d_1(f_1, f_2)$ equals zero, but $d_0(f_1, f_2)$ is positive. See also a similar case in Fig. 2, where two different splines are shown, with large d_0 distance, $d_0(f_1, f_2) = 112.8$, but relatively small d_1 distance, $d_1(f_1, f_2) = 1.56$.

3. Results

EPs were recorded daily from an awake rat for 14 days (6 for Control, 8 for SS). Instead of obtaining 42 intensity-series in response to the three sounds, we obtained only 38 of them (13 for each of the two tone bursts, 12 for click). All the missing series (four) were in the SS group, mainly due to animal's restless behavior known to associate with SS-overdoses.

3.1. General properties of single-trial auditory EPs in individual sessions

In a given session, the 79 trials of EPs we had analyzed showed noticeable inter-trial variations regarding both the time-waveform and the background activity (see Fig. 1).

At a given stimulus level, single-trial EP integrals did not distribute symmetrically around the median. Across the intensity range, EP integrals appeared larger in the SS groups, especially with loud sounds (e.g., > 45 dB SPL). Such enhanced responses to sound are consistent with the hyperacusis reported with the SS-induced tinnitus.

3.2. Differences in the auditory EP across daily intensity series

Each intensity-series, which consisted of 19 sessions, was collected in response to each sound at a different day. Across these days, the changes in the

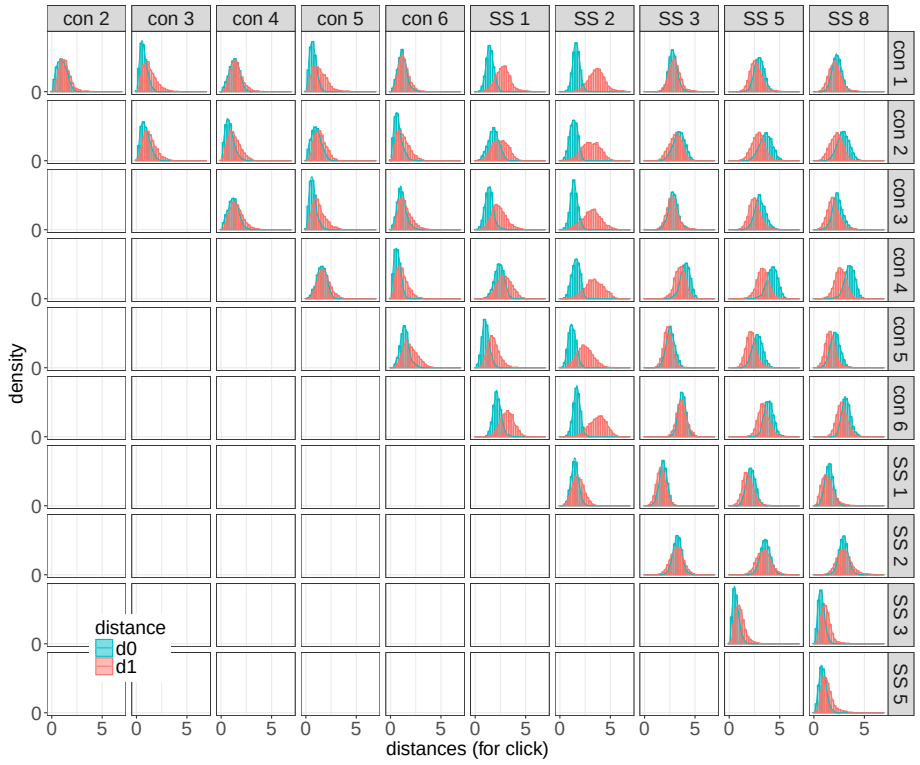

Figure 5: Histograms of the d_0 and d_1 cross-distance measures computed between the spline curves from all intensity-series obtained in response to the click sound. Positions of the subplots are same as in Fig. 4.

response-level functions (derived from the intensity series) depended not only on the experimental condition (Control or SS), but also on which form the responses were represented, i. e., which distance (d_0 or d_1) was used for the quantification of the similarity. In the SS group, results from d_0 representation showed larger inter-series variations (in terms of median-disparity in the cross-distance distributions), compared with the more consistent results in the Control group. Such inter-series disparities appeared even larger when compared in their d_1 representations. The inter-series comparisons were done based on d_0 and d_1 distances: between member-series both within and across the SS or Control groups. To facilitate viewing, we display the results in a pixel plot, see Fig. 4, with a temperature-color code (or heatmap, with redder color for larger similarity, brighter color for smaller similarity). The two axes of the plot give labels to the member-series in both the Control and SS groups in the chronological order. The medians of the cross-distances are calculated for all possible comparisons between any two member-series. Fig. 5 shows the corresponding cross-distance histograms of Fig. 4. In the Control group, the cross-distance histograms invariably show smaller inter-series disparity (regardless of the representation in d_0 or d_1). Whereas in d_1 (but not in d_0) SS member-series showed a clearer separation from the Controls as a group. The complete results are depicted in Supplementary Figs. S3, S4 and S5.

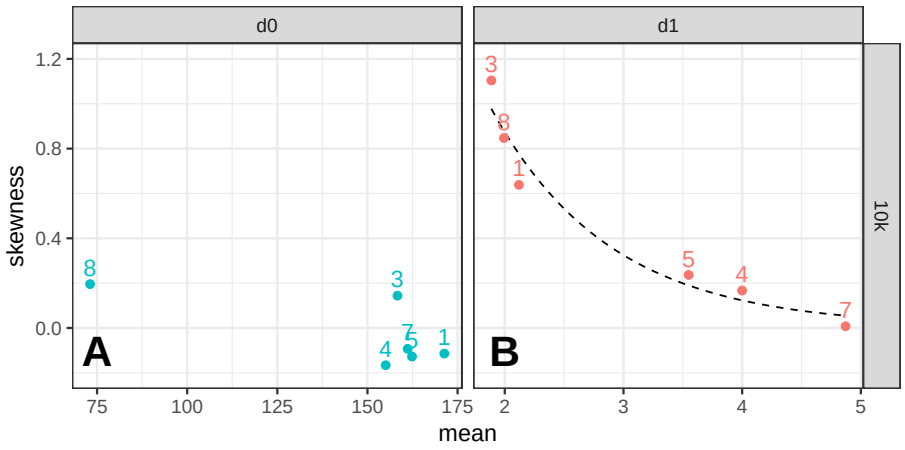

Figure 6: Relationship between the skewness and the mean of the cross-distance distribution (based on EP obtained in response to 10 kHz tone of the SS series compared with Controls) showing results from two different representations: (A) distribution of the d_0-cross-distances, and (B) distribution of the d_1-cross-distances. Each symbol represents results from an intensity-series recorded on the day as labeled by the numerals. Data-points in (B) are curve-fitted (dash line) to show the apparent inverse (exponentially decreasing) relationship.

3.3. Differences in responses at high sound intensities

Since SS is known to produce hyperacusis to loud sounds, we further examined responses obtained at the high intensity region (50 to 75 dB SPL). For cross-comparison with SS, all Control spline curves were first pooled together (as their EP responses were more stable). Aspects of cross-distance measures were displayed on a scatter-plot in terms of the mean and skewness of the distributions, see Fig. 6 and Supplementary Fig. S6. Note that d_1 data-points from different series form a reverse-relationship (or grossly an exponential decay function, see the dashed line in Fig. 6B). In simple words, the smaller the mean deviation from the Control, the greater the skewness of the cross-distance distribution. For tonal responses, this apparent relationship was more obvious with the representation in d_1 and less so in d_0. Interestingly, no similar relationship was found in the scatter-plots of other intensity segments (whole or intermediate intensity region). We also tested other statistical parameters (like coefficient of variance, kurtosis) and did not find such relationships (data not shown).

In summary, in comparison with the more conventional approach of characterizing the similarity of the EP response-level functions by the d_0 distance, its quantification by the d_1-distance provided finer details on the SS effects. When plotted in a cross-distance histogram against the Controls, see Fig. 7, clearer separation in results was seen not only between Control and SS groups, but also among member-series of the more variable SS group.

4. Discussion

The principal findings of the present study on auditory EPs are: (a) multiple response-level functions (splines from sets of single-trial EP integrals across

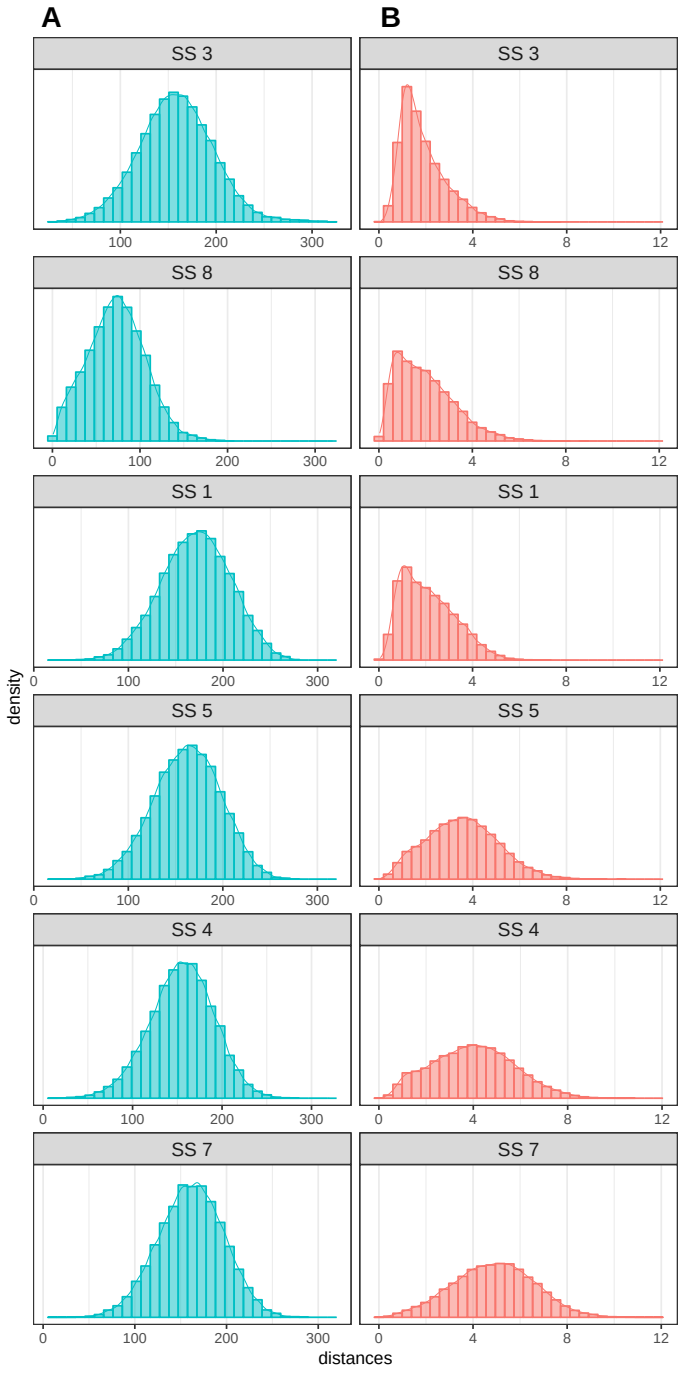

Figure 7: Histograms of the d_0-cross-distances (column A) and d_1-cross-distances (column B) computed between the curves of SS group-members and the curves of the pooled control groups in response to 10 kHz tone. The panels are arranged from top to bottom according the descending order of the member-series along-side the exponential dashed line in Fig. 6B.

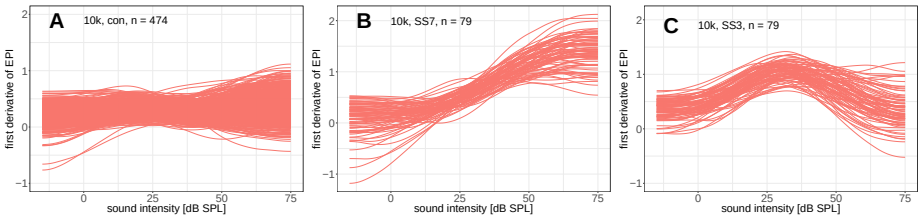

Figure 8: The first-derivative representation of the EP integral (EPI) functions in response to 10 kHz tone overlaid for (A) the Control, (B) SS day-7, and (C) SS day-3. Comparing SS-3 with SS-7, note the big difference in their disparities with Control, particularly at the high intensity region (50 to 75 dB SPL).

stimulus-intensities) provided more information on the SS-effects, when compared to the traditional approach of single averaged response-level functions; (b) FDA allowed the comparison (or better separation) of response-level functions obtained over different days based on cross-difference measures; (c) response-level functions of the SS group were separated from the Control in a way clearer, when they were compared in the form of the d_1-distance, than in the d_0-distance; (d) SS-effects not only varied with sound types (tone or click), but also with responses at high intensities in line with the known SS effects. Within this high-intensity region, an inverse relationship was found over daily recordings between two simple statistical parameters of their cross-difference histograms, viz., the mean and the skewness.

That multiple response-level functions from single trials were more informative than a single averaged response-level function is not surprising. Since additional information from the statistics of the cross-difference histograms could be used to reveal the SS effects. What remains unexplored is the importance of the order in which single-EP integrals were selected from sessions across intensities for a given stimulus. We are unable to rule out any history effects that could have affected the EP responses, or whether spline curves are independent of one another. However, such possible bias, if present, would not violate the assumptions of the FDA. Since the main feature of such type of spline data is linked with the dependence of structure existed between the statistical units (Ferraty et al., 2006). An alternative experiment is to present sound stimuli in a manner that is randomized in intensity (rather than the systemic change from low to high as in this study). We have some preliminary data to show the presence of minor history effects which did not compromise the conclusions we have made.

We found in general cross-distance comparison was more powerful in separating group-members when represented in the form of d_1-distance which reflected more clearly the dynamic range in the response level function. Since under SS treatment, more neurons were likely recruited into activation (presumably by the elevated central gain), the dynamic range or its change in the response-level function would then be depicted more clearly in the representation of the first derivative of the EP integral, i. e., when comparing in the form of the d_1-distance. That the dynamic range was altered under SS treatment is consistent with our previous observations on a larger number of animals (Wan et al., 2015). Furthermore, our present finding of SS effects in the high frequency region (10 to 16 kHz) is also in line with the literature on hyperacusis (Chen et al., 2013).

The advantage of d_1-distance over d_0-distance was seen more clearly for

responses to tones than to click. This could be related to the differences in the spectral and temporal properties of the sounds (like band-width and onset time) and how these stimulus features are processed in the auditory system. Tones are narrow-band stimuli which activate small number of neurons that sensitive those frequencies in the tonotopic array. With small number of neurons involved, response-level functions were typically small (see Control conditions in Supplementary Figs. S1 and S2). On the other hand, a broad-band signal like click (an acoustic transient with a duration 0.01 msec, much less than the 2.5 msec rise-time of tone bursts), could have driven more auditory neurons into synchronized activity. Consequently, responses were larger even in the Control conditions (see Supplementary Figs. S1 and S2). As the dynamic range was already visible in the spline representation, it is not too surprising that the advantage of the first-derivative representation appeared less in the click data compared with tones.

Our finding on the SS effects on click is also consistent with our earlier report using more traditional approach (Wan et al., 2015). In that study, we had reported the large inter-series variations which we also observed in the present study. Such temporal variations could be explained in part by the SS effects that were expressed differentially during the several hours time course after drug-administration in each day of the experiment, and also the accumulation of the drug effects from a previous day. That we were able to reveal such subtle changes in EP responses over short periods of time would make our present FDA approach a powerful tool in neuropharmacology for the detailed study of drug effects on brain activities.

The observation of an inverse relationship on the mean-skewness plot based on cross-distance comparisons at the loud sound region is interesting and worth some discussion. In Fig. 6, let us consider two marginal cases (SS-3 and SS-7) in the d_1-distance results, together with their corresponding histograms in Fig. 7. The origin of such inverse relationship could reside in the different temporal actions of SS over time (in the same or different days). The different actions particularly at the high intensity region where SS effects are well-known (hyperacusis), could be reflected in the shape of the first-derivative curves, see Fig. 8. The curves of SS-3 at this high-intensity region are more variable than SS-7. Moreover, SS-3 also has more overlap with the Control than SS-7. Such disparities could well contribute to their differences in the skewness.

Acknowledgments

We thank Dr. Paul Poon for reading the manuscript and for helpful discussion. This work was supported by the grant GA15-06991S of the Czech Science Foundation, the Ministry of Science and Technology (103-2221-E-039-007-MY3) and Taiwan-Czech bilateral project (MOST-GACR: 105-2923-B-009-001-MY3).

References

Alho, K., 1992. Selective attention in auditory processing as reflected by event-related brain potentials. Psychophysiology 29 (3), 247–263.

Benhenni, K., Ferraty, F., Rachdi, M., Vieu, P., 2007. Local smoothing regression with functional data. Computational Statistics 22 (3), 353–369.

Bernasconi, F., De Lucia, M., Tzovara, A., Manuel, A. L., Murray, M. M., Spierer, L., 2011. Noise in brain activity engenders perception and influences discrimination sensitivity. Journal of Neuroscience 31 (49), 17971–17981.

Bidelman, G. M., 2017. Amplified induced neural oscillatory activity predicts musicians' benefits in categorical speech perception. Neuroscience.

Boettcher, F. A., Salvi, R. J., 1991. Salicylate ototoxicity: review and synthesis. American journal of otolaryngology 12 (1), 33–47.

Cazals, Y., 2000. Auditory sensori-neural alterations induced by salicylate. Progress in neurobiology 62 (6), 583–631.

Chen, G.-D., Stolzberg, D., Lobarinas, E., Sun, W., Ding, D., Salvi, R., 2013. Salicylate-induced cochlear impairments, cortical hyperactivity and re-tuning, and tinnitus. Hearing research 295, 100–113.

Coles, R., 1984. Epidemiology of tinnitus:(1) prevalence. The Journal of Laryngology & Otology 98 (S9), 7–15.

Craven, P., Wahba, G., 1978. Smoothing noisy data with spline functions. Numerische Mathematik 31 (4), 377–403.

Faisal, A. A., Selen, L. P., Wolpert, D. M., 2008. Noise in the nervous system. Nature reviews neuroscience 9 (4), 292–303.

Ferraty, F., Mas, A., Vieu, P., 2006. Advances on nonparametric regression for functional variables. arXiv preprint math/0603084.

Ferraty, F., Vieu, P., 2006. Nonparametric functional data analysis: theory and practice. Springer.

Hastie, T. J., Tibshirani, R. J., 1990. Generalized additive models. Vol. 43. CRC Press.

Heller, A. J., 2003. Classification and epidemiology of tinnitus. Otolaryngologic Clinics of North America 36 (2), 239–248.

Jastreboff, P. J., 1990. Phantom auditory perception (tinnitus): mechanisms of generation and perception. Neuroscience research 8 (4), 221–254.

Langguth, B., Kreuzer, P. M., Kleinjung, T., De Ridder, D., 2013. Tinnitus: causes and clinical management. The Lancet Neurology 12 (9), 920–930.

Levi, H., Chisin, R., 1987. Can tinnitus mask hearing? A comparison between subjective audiometric and objective electrophysiological thresholds in patients with tinnitus. Audiology 26 (3), 153–157.

Mas, A., Pumo, B., 2009. Functional linear regression with derivatives. Journal of Nonparametric Statistics 21 (1), 19–40.

Neri, P., 2010. How inherently noisy is human sensory processing? Psychonomic Bulletin & Review 17 (6), 802–808.

Noreña, A. J., 2011. An integrative model of tinnitus based on a central gain controlling neural sensitivity. Neuroscience & Biobehavioral Reviews 35 (5), 1089–1109.

Noreña, A. J., Farley, B. J., 2013. Tinnitus-related neural activity: theories of generation, propagation, and centralization. Hearing research 295, 161–171.

Qiu, W., Chang, C., Liu, W., Poon, P. W. F., Hu, Y., Lam, F. K., Hamernik, R. P., Wei, G., Chan, F. H. Y., 2006. Real-time data-reusing adaptive learning of a radial basis function network for tracking evoked potentials. IEEE Transactions on Biomedical Engineering 53 (2), 226–237.

Ramsay, J., Silverman, B. W., 2005. Functional Data Analysis, 2nd Edition. Springer Series in Statistics. Springer.

Ramsay, J. O., 1982. When the data are functions. Psychometrika 47 (4), 379–396.

Ramsay, J. O., 1988. Monotone regression splines in action. Statist. Sci. 3 (4), 425–441.

Ramsay, J. O., Dalzell, C. J., 1991. Some tools for functional data analysis. Journal of the Royal Statistical Society. Series B (Methodological) 53 (3), 539–572.

Reinsch, C. H., 1967. Smoothing by spline functions. Numer. Math. 10, 177–183.

Roberts, L. E., Eggermont, J. J., Caspary, D. M., Shore, S. E., Melcher, J. R., Kaltenbach, J. A., 2010. Ringing ears: the neuroscience of tinnitus. Journal of Neuroscience 30 (45), 14972–14979.

Ullah, S., Finch, C. F., 2013. Applications of functional data analysis: A systematic review. BMC Med. Res. Methodol. 13 (43).

Wan, I., Pokora, O., Chiu, T., Lansky, P., Poon, P. W., 2015. Altered intensity coding in the salicylate-overdose animal model of tinnitus. BioSystems 136, 113–119.

Wang, J.-L., Chiou, J.-M., Müller, H.-G., 2016. Functional data analysis. Annual Review of Statistics and Its Application 3 (1), 257–295.

Supplementary figures

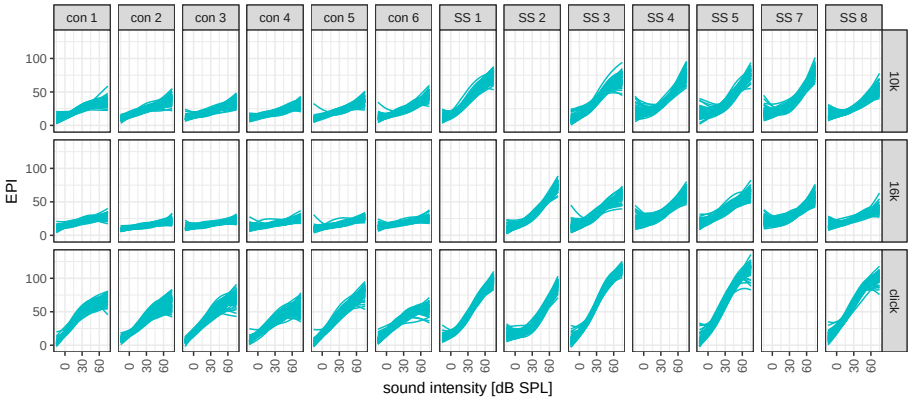

Figure S1: Response-level functions (superposition of spline-fitted curves that constitute a complete intensity-series) showing their shapes in dependency on the sound intensity. Responses represent single-trial EP integrals (EPI) to tone burst 10 kHz, 16 kHz and to clicks for Control groups (con, day-1 to day-6) and salicylate overdose groups (SS, day-1 to day-8).

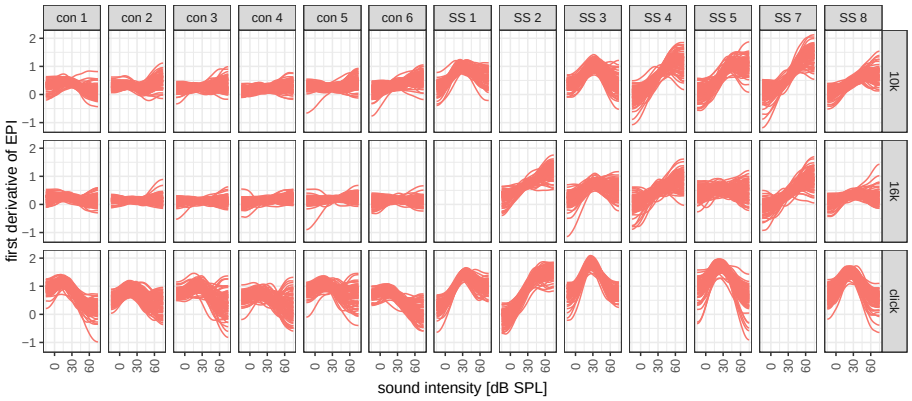

Figure S2: First derivatives of the splines from Supplementary Fig. S1.

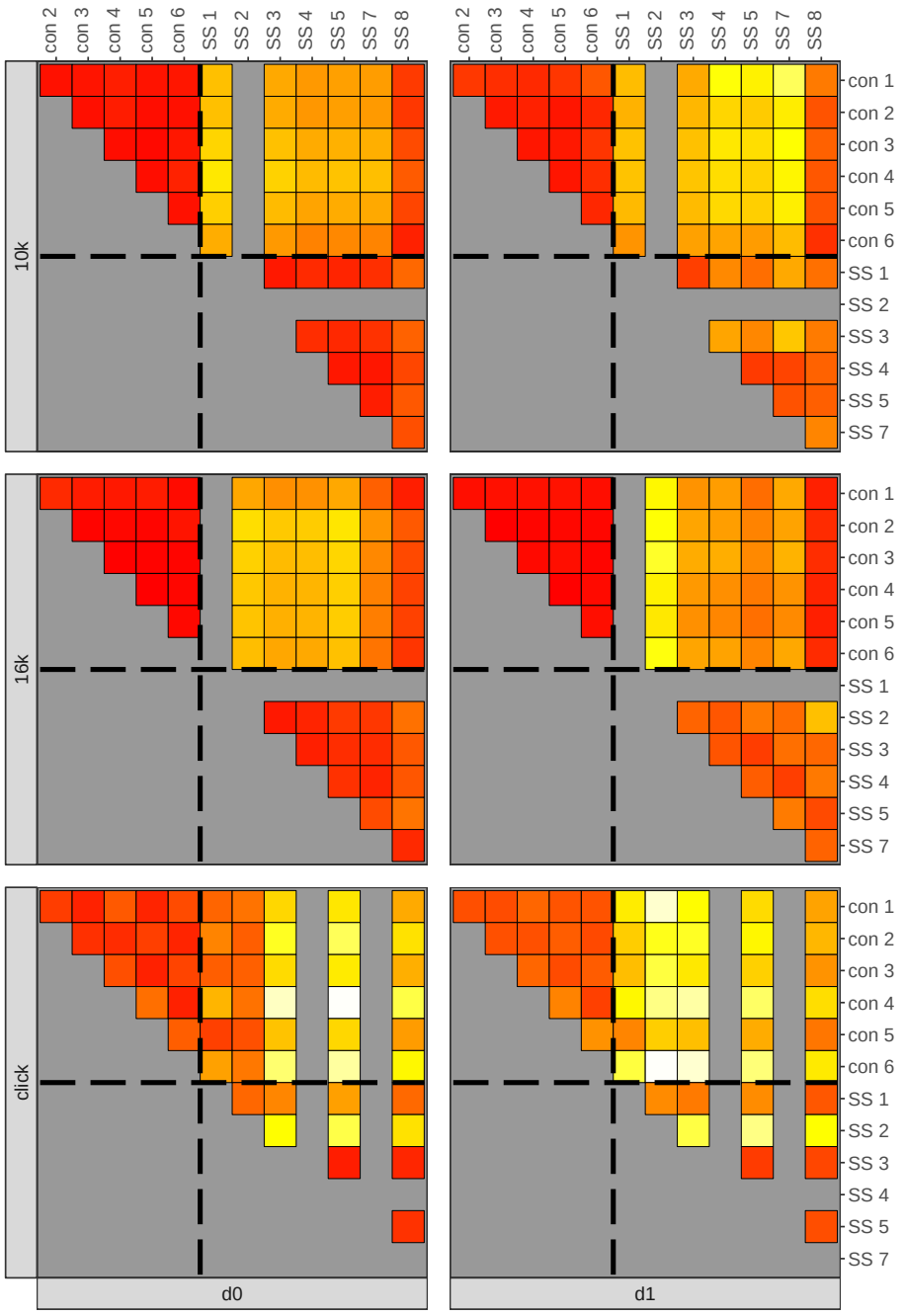

Figure S3: Pixel plots (or heatmaps) showing the results of the inter-series comparison between any two group-members of the Control and SS, color-coding median-disparity cross-distances histograms (redder color means larger similarity, brighter color means smaller similarity). Data are from tone bursts 10 kHz, 16 kHZ and click responses: for Control and SS conditions, numerals on axes indicate the days of recording, and are arranged chronologically. (left column) Heatmap of the results on d_0-cross-distances computed between pairs curves for all group-members. (right column) Heatmap of results on d_1-cross-distances for the same data as in the left column. Dashed lines divide the Control and SS groups for easy viewing. The corresponding cross-difference histograms are shown in Fig. 5 and Supplementary Figs. S4 and S5.

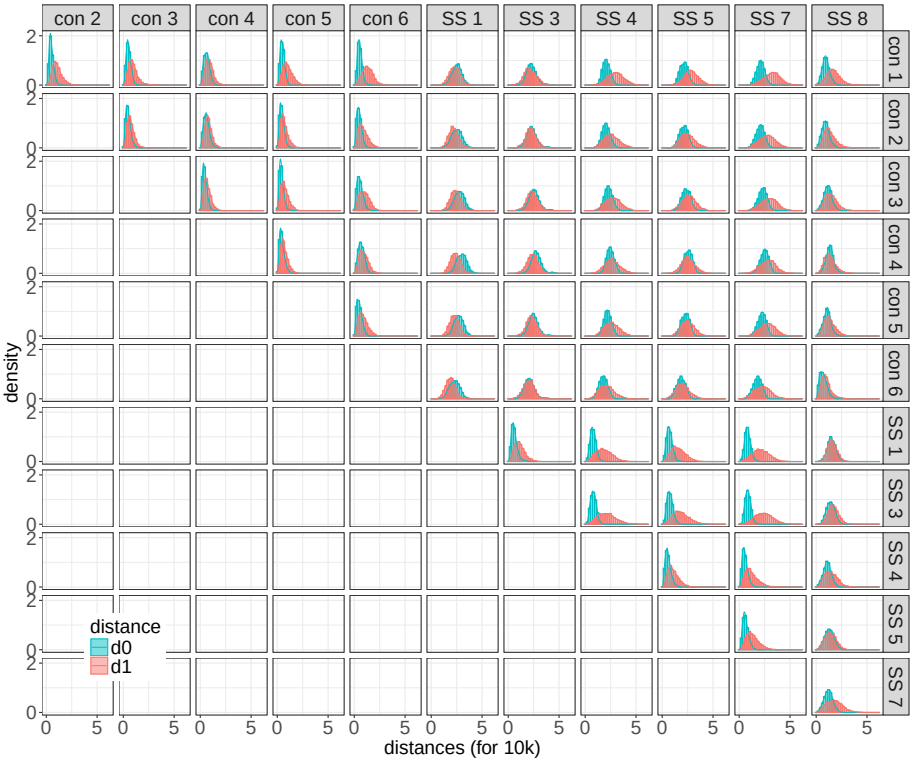

Figure S4: Histograms of the d_0 and d_1 cross-distance measures computed between the spline curves from all intensity-series obtained in response to the 10 kHZ tone bursts. Positions of the subplots are same as in Fig. S3.

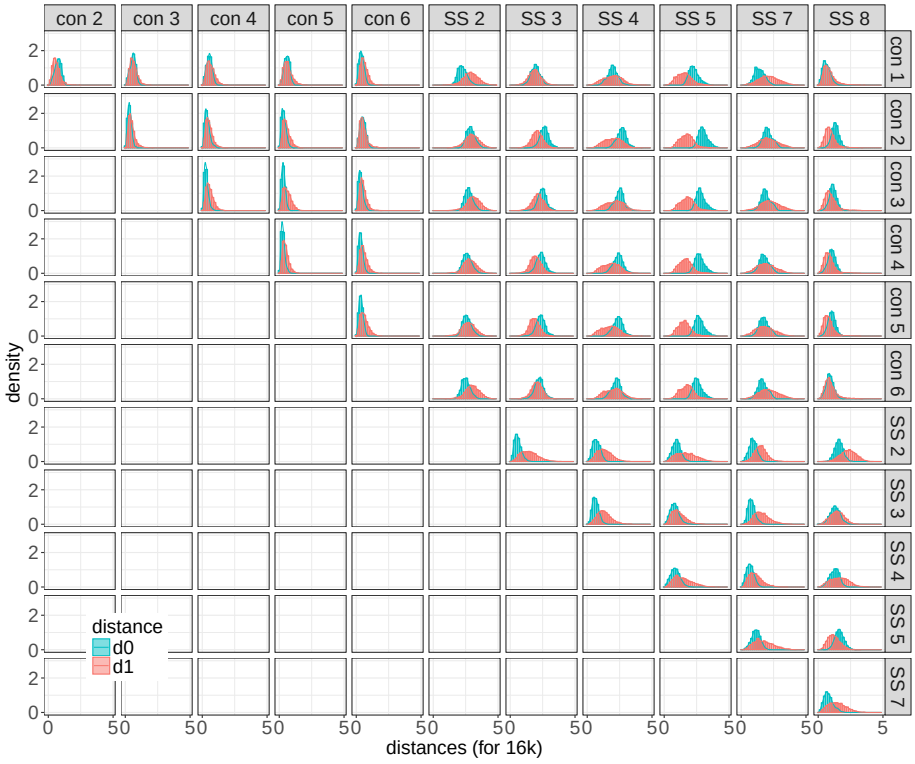

Figure S5: Histograms of the d_0 and d_1 cross-distance measures computed between the spline curves from all intensity-series obtained in response to the 16 kHZ tone bursts. Positions of the subplots are same as in Fig. S3.

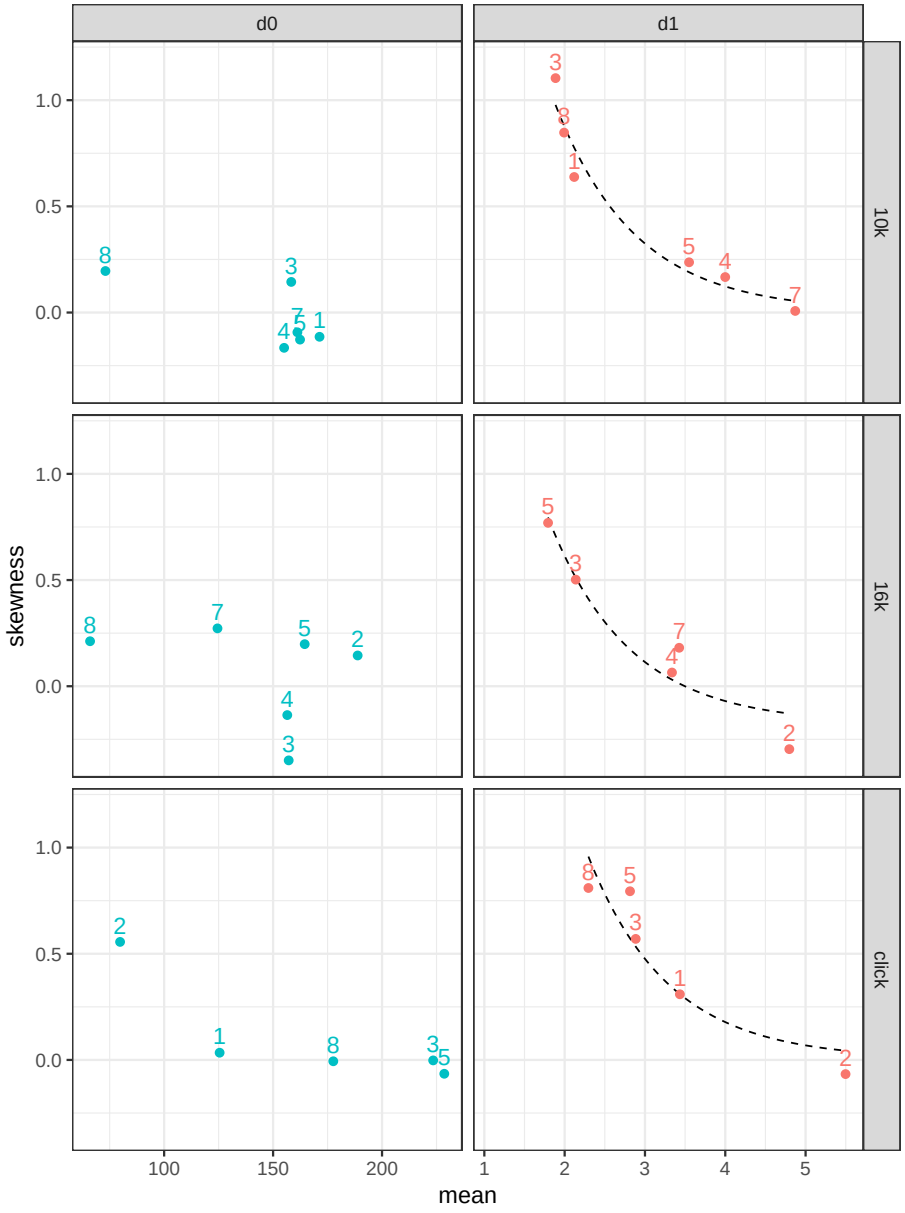

Figure S6: Relationship between the skewness and the mean of the cross-distance distribution (based on EP obtained in response to 10 kHz and 16 kHZ tone bursts and to clicks of the SS series compared with Controls) showing results from two different representations: (left column) distribution of the d_0-cross-distances, and (right column) distribution of the d_1-cross-distances. Each symbol represents results from an intensity-series recorded on the day as labelled by the numerals. Data-points in the right column are curve-fitted (dash line) to show the apparent inverse (exponentially decreasing) relationship.